

## Data from Temperature-Programmed Desorption (TPD) to Check New Aspects of Ammonia Synthesis on Iron Catalysts

### I. The TPD of Adsorbed Hydrogen on Iron Catalysts and Active States<sup>1</sup>

KAI-HUEI HUANG, XIAO-MING ZENG, AND JI-TAO LI

P.O. Box 276, Department of Chemistry and Institute of Physical Chemistry,  
Xiamen University, Xiamen, China

Received February 22, 1982; revised November 2, 1982

The temperature-programmed desorption spectra of hydrogen on  $K_2O$ - $CaO$ - $Al_2O_3$ -Fe,  $CaO$ - $Al_2O_3$ -Fe,  $Al_2O_3$ -Fe catalysts at normal atmospheric pressure and various temperatures have been obtained. Desorption peaks are observed in three temperature intervals, namely, 120-170, 280-380, and 480-540°C. Having studied the changes in the TPD spectra effected by adsorbed nitrogen, promoters, and adsorption conditions, we characterized these peaks as  $H_2^{\delta+}$ ,  $H^{\delta+}$ , and  $H^{\delta-}$ , respectively. The effect of promoters and dipole-dipole mutual interaction energy have been estimated. The dynamically induced adsorption models for the synthesis of ammonia on doubly promoted iron catalysts proposed by K. H. Huang ("Proceedings, 7th International Congress on Catalysis," p. 554, 1981; *Sci. Sin.* 24, No. 6 (1981); *Universitatis Amoiensis (Acta Sci. Natur.)* 3, 112, 130 (1978)) have been further supported and extended. The adsorption equilibrium constants have been estimated using a statistical thermodynamic method. The results established that  $(K_{H_2}P_{H_2})_{H^{\delta+}}$  and  $(K_{H_2}P_{H_2})_{H_2^{\delta+}}$  are much less than unity as was assumed in the previous derivation of the kinetic equation (K. H. Huang, *Sci. Sin.* 24, No. 6 (1981)). This equation has been proved.

### INTRODUCTION

The mechanism of ammonia synthesis on iron catalysts is of fundamental importance. Despite extensive experimental work and much thought, the mechanism of ammonia synthesis has not yet been fully elucidated. Recently, attention has been focused on activation of  $N_2$  passes through a molecularly adsorbed species and whether hydrogen participates in the process of dissociation of  $N_2$  on doubly promoted catalysts (1).

The adsorption of hydrogen has been classified by the temperatures at which maxima appear in the isobaric adsorption into three types, A, B, and C, with the maxima at -90, 100, and -196°C, respectively (2). However, as we will show below, more than one adsorption state may occur simultaneously at the same temperature, the

same pressure, and on the same catalyst. In our opinion, the isobaric adsorption alone is not adequate for classifying the adsorption states. Wedler and Borgmann observed only the  $\beta$ -type of adsorbed hydrogen in TPD from iron films (3), but no promoters were present and the temperature and pressure were lower than in TPD studies from conventional catalysts. Amenomiya and Pleizier noted two adsorption peaks between room temperature and 200°C on a promoted catalyst (Haldor Topsøe Type KMI  $K_2O$ - $CaO$ - $MgO$ - $Al_2O_3$ -Fe) (4) and they characterized both peaks as representing  $\beta$ -type adsorption.

The mutual interaction between simultaneously adsorbed  $N_2$  and  $H_2$  has been observed by several authors. All experiments were run at less than 1 atm, and moreover, in the case of doubly promoted iron catalyst there were some controversial results. For example, Emmett *et al.* (5) and Amenomiya *et al.* (4) found nitrogen would displace hydrogen adsorbed in the  $\beta$  form,

<sup>1</sup> The paper was presented at 182nd ACS National Meeting, August 27, 1981.

whereas Bokhoven *et al.* (6) found that when the nitrogen was preadsorbed, there was an increase in the amount of chemisorption of hydrogen at 168 and 220°C. They explained this as a  $H^+$  and  $N^-$  reaction and proposed an adsorption heat  $Q_{H^+}$  larger than  $Q_{H^-}$  (but our result is  $Q_{H\delta^+}$  smaller than  $Q_{H\delta^-}$ ). Tamaru *et al.* (7) also found that the adsorption amount of both  $N_2$  and  $H_2$  were increased when  $N_2$  and  $H_2$  were adsorbed simultaneously at 450 and 500°C. The rate of ammonia synthesis is proportional to the pressure of  $H_2$  at a constant amount of nitrogen preadsorbed and at a low hydrogen pressure (3–20 cm Hg). It is difficult to explain the correlation of the rate of ammonia synthesis with the total amount of adsorbed hydrogen if we do not divide the adsorption into active and inactive species. The experimental results of Topsøe *et al.* (8) showed there is no clear correlation between the amount of adsorbed hydrogen and the activity for ammonia synthesis. Wedler and Borgmann (3) studied adsorption of hydrogen and of nitrogen on iron films at low temperatures and the adsorption of hydrogen on films containing adsorbed nitrogen. They believed that adsorbed nitrogen was displaced by hydrogen. However, as we will show (1d), the amount of adsorbed  $N_2^{\delta-}$  is increased if nitrogen and hydrogen are coadsorbed on doubly promoted iron catalyst during cooling from 400°C to low temperature. Huang (1) has advanced a hypothesis for the nature of active site and nitrogen and hydrogen adsorbed on it. To further support this, we have observed the TPD spectra of hydrogen at atmospheric pressure as affected by the preadsorbed nitrogen, promoters, and the conditions of adsorption.

## EXPERIMENTAL

### 1. Apparatus and Method

The apparatus used in the TPD spectra and desorption peaks analysis is shown in Fig. 1.

High-purity gas or carrier gas (Ar or He) passes through columns 3, 4, 5, and 6 to remove  $H_2O$  and  $O_2$ . It then passes through the six-way valve 13 and the catalyst bed 15 to reach the thermal conductivity cell 10A. To analyze the components in the exit gas, the gas from 10A is passed through the six-way valve 14 and the sample tube 16 to the thermal conductivity cell 11B.

After exposure of the catalysts to hydrogen or nitrogen, the residual adsorptive was removed by a flow of argon before starting a TPD run.

Where two peaks appear in TPD with some overlapping, the temperature rise was interrupted just after the maximum in the earlier peak until the signal had decreased considerably. The temperature rise was then restarted. This procedure led to better resolution of the two peaks.

### 2. Catalyst Composition (Unreduced)

Catalyst I: 0.7%  $K_2O$ –1.5%  $CaO$ –2.3%  $Al_2O_3$ – $Fe_3O_4$ .

Catalyst II: 1.7%  $CaO$ –2.2%  $Al_2O_3$ – $Fe_3O_4$ .

Catalyst III: 2.3%  $Al_2O_3$ – $Fe_3O_4$ .

The catalysts were kindly furnished by Mr. Wei Ke Mei (Fuchow University). They were prepared by the industrial fusion method.

### 3. Procedure for Reduction

The reduced catalyst was heated in an oven for 1 hr at 120°C, 0.5 g of catalyst was put into the microreactor for TPD. The system was evacuated for 2 hr, and the catalyst was then reduced in a hydrogen stream (flow rate 50  $cm^3/min$ ). The reducing conditions (heating rate, reduction time, controlled temperature) are the same as those of industrial catalysts, as shown in Fig. 2.

### 4. Gas Chromatographic Analysis

Chromatograph: Model GC-103, Shanghai.

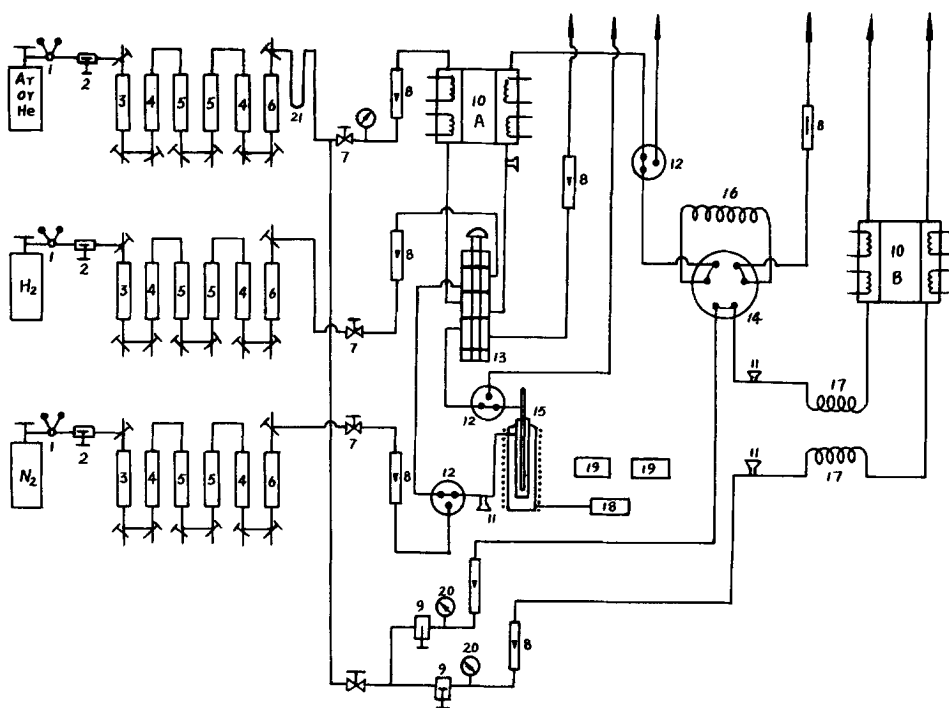


FIG. 1. The schemetic diagram of TPD experiment. (1) Reduction valve, (2) flow rate controller, (3) silica gel, (4) 5-Å molecular sieve, (5) Ni deoxidizer, (6) MnO deoxidizer, (7) valve for stabilizing pressure, (8) rotameter, (9) valve for stabilizing flow, (10A) gas chromatograph Model 102, (10B) gas chromatograph Model 103, (11) sample injection inlet, (12) three-way valve, (13) six-way valve, (14) plane type six-way valve, (15) microreactor (desorption cell), (16) sample tube, (17) chromatographic column, (18) temperature-programmed controller, (19) double-pen recorder, (20) pressure meter, (21) liquid air cold trap.

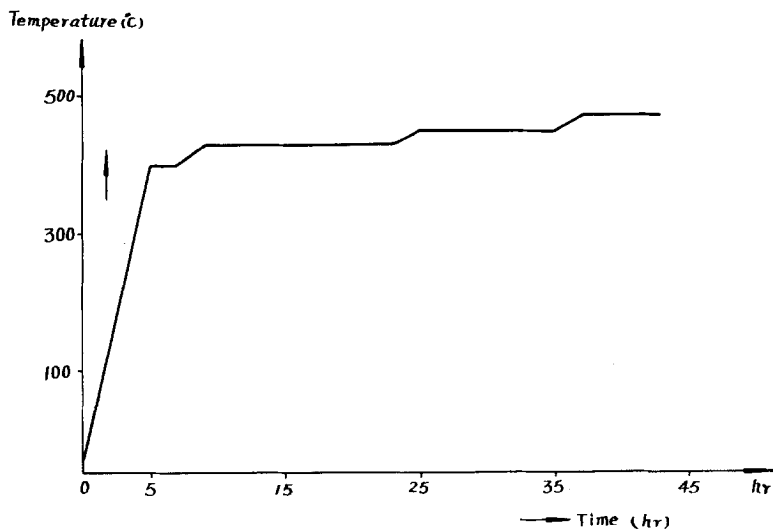


FIG. 2. The reduction curve of iron catalysts.

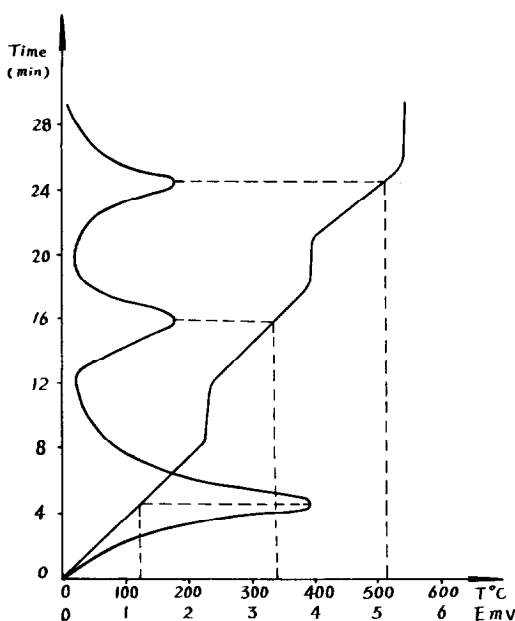


FIG. 3. The TPD spectra of catalyst I ( $\text{K}_2\text{O}-\text{CaO}-\text{Al}_2\text{O}_3-\text{Fe}$ ) with  $\text{H}_2$  adsorbed during cooling from 400 to  $\sim 20^\circ\text{C}$ .

Chromatographic column: 3-mm diameter, 2 m long, 5-Å molecular sieve (32–45 mesh).

Temperature of column:  $60^\circ\text{C}$ .

Temperature of detector chamber:  $60^\circ\text{C}$ .

Detection limit: 40 ppm.

#### EXPERIMENT RESULTS

##### 1. TPD of Hydrogen Adsorbed on Iron Catalysts During Cooling from $400^\circ\text{C}$ to Room Temperature ( $20^\circ\text{C}$ )

After the catalyst had been well reduced at  $400^\circ\text{C}$  by an  $\text{H}_2$  stream ( $50 \text{ cm}^3/\text{min}$ ) passing through the catalyst bed, the temperature was decreased slowly from  $400^\circ\text{C}$  to room temperature. Then, the carrier gas Ar ( $70 \text{ cm}^3/\text{min}$ ) was passed through the catalyst bed to sweep out residual hydrogen gas until no hydrogen could be detected by the gas chromatograph in the exit gas and the baseline of the gas chromatograph had become stable. The TPD spectrum was then observed at a heating rate of  $25^\circ\text{C}/\text{min}$  and a carrier gas flow rate of  $70 \text{ cm}^3/\text{min}$  on cata-

lysts I, II, and III. These spectra are shown in Figs. 3, 4, and 5, respectively.

##### 2. TPD of Hydrogen Adsorbed at Room Temperature

The well-reduced catalyst was heated in flowing argon several times from 20 to  $500^\circ\text{C}$  until no hydrogen peak could be seen in the gas chromatograph. It was cooled to room temperature and hydrogen stream ( $50 \text{ cm}^3/\text{min}$ ) was passed through the catalyst bed until the catalyst was fully saturated. The next steps were the same as described in section 1. TPD spectra on catalysts I, II, and III are shown in Figs. 6, 7, and 8, respectively.

##### 3. TPD Spectra of $\text{H}_2$ and $\text{N}_2$ Coadsorbed at Room Temperature

Hydrogen was desorbed from the well-reduced catalyst as described in section 2.  $\text{N}_2$  ( $70 \text{ cm}^3/\text{min}$ ) and  $\text{H}_2$  ( $70 \text{ cm}^3/\text{min}$ )

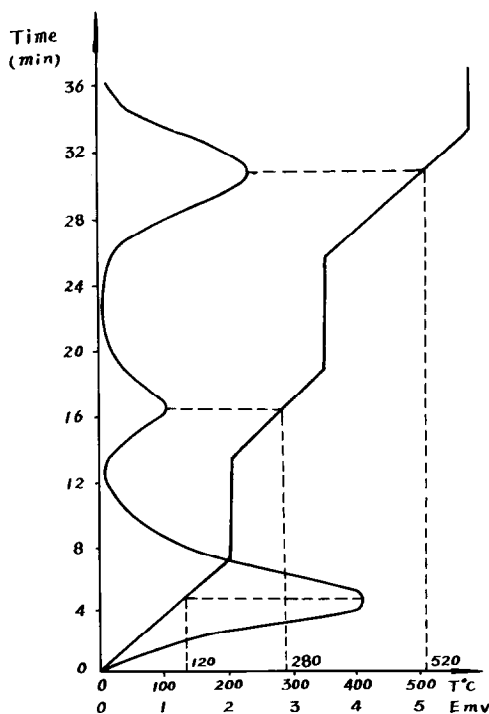


FIG. 4. The TPD spectra of catalyst II ( $\text{CaO}-\text{Al}_2\text{O}_3-\text{Fe}$ ) with  $\text{H}_2$  adsorbed during cooling from 400 to  $\sim 20^\circ\text{C}$ .

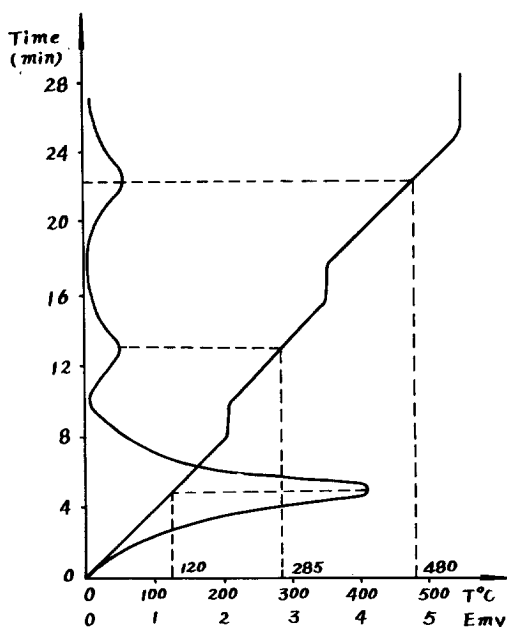


FIG. 5. The TPD spectra of catalyst III ( $\text{Al}_2\text{O}_3\text{-Fe}$ ) with  $\text{H}_2$  adsorbed during cooling from 400 to  $\sim 20^\circ\text{C}$ .

streams were passed alternately through the catalyst bed at intervals of 5 min until saturation was reached. Then TPD was carried out as described in paragraph 1. The TPD on catalysts I, II, and III are shown in Figs. 9, 10, 11, respectively.

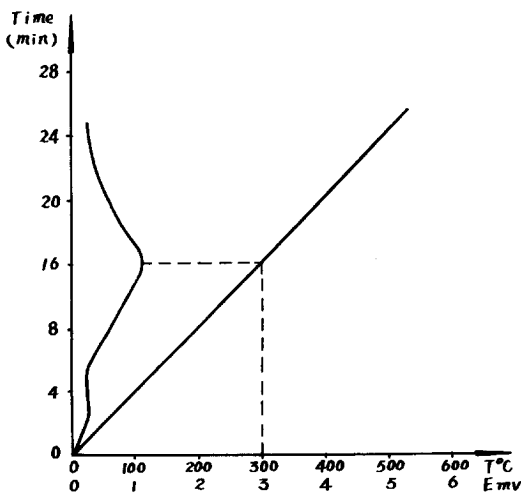


FIG. 6. The TPD spectra of catalyst I ( $\text{K}_2\text{O-CaO-Al}_2\text{O}_3\text{-Fe}$ ) after exposure to  $\text{H}_2$  at  $\sim 20^\circ\text{C}$ .

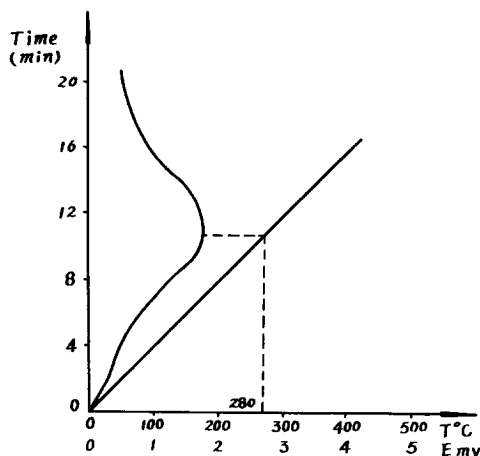


FIG. 7. The TPD spectra of catalyst II ( $\text{CaO-Al}_2\text{O}_3\text{-Fe}$ ) after exposure to  $\text{H}_2$  at  $\sim 20^\circ\text{C}$ .

#### 4. Displacement of Strongly Adsorbed Hydrogen by $\text{N}_2$ at 510, 410, and $20^\circ\text{C}$

Catalyst after reduction in  $\text{H}_2$  at  $400^\circ\text{C}$  was heated twice in flowing Ar from 20 to  $550^\circ\text{C}$ . The temperature was then adjusted to 510 or  $410^\circ\text{C}$  and no hydrogen could be detected in the exit gas. The argon flow gas was replaced by one of nitrogen, and as shown in Fig. 12a, hydrogen appeared in the exit nitrogen. If  $\text{N}_2$  and Ar streams were passed alternately through the catalyst bed, changes in hydrogen concentration in the

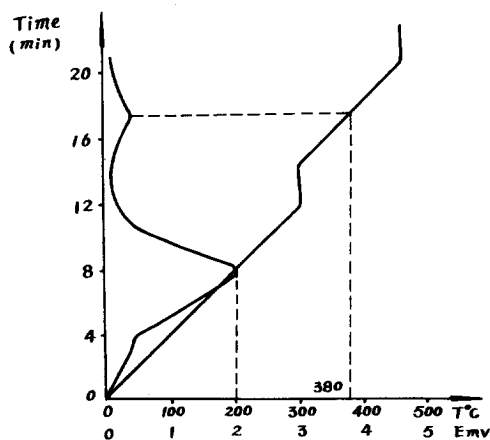


FIG. 8. The TPD spectra of catalyst III ( $\text{Al}_2\text{O}_3\text{-Fe}$ ) after exposure to  $\text{H}_2$  at  $\sim 20^\circ\text{C}$ .

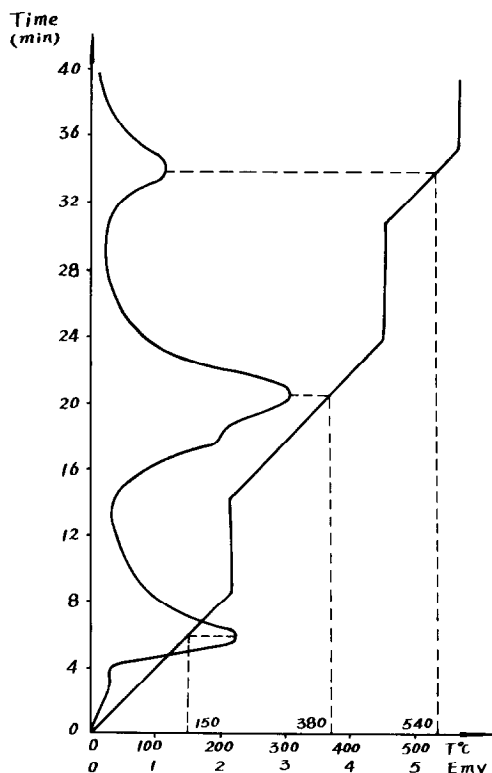


FIG. 9. TPD spectra on catalyst I ( $\text{K}_2\text{O}-\text{CaO}-\text{Al}_2\text{O}_3-\text{Fe}$ ) after coadsorption of  $\text{H}_2$  and  $\text{N}_2$  at  $\sim 20^\circ\text{C}$ .

exit gas were observed as shown in Fig. 12b. It is clear that adsorbed hydrogen could be displaced by adsorbed nitrogen but not by the inert Ar.

After reduction of a catalyst followed by desorption of  $\text{H}_2$  as described above, a flow of  $\text{N}_2$  was established over the catalyst at  $\sim 20^\circ\text{C}$ . The procedure described in section 1 was followed and the TPD spectra obtained on catalysts I and II are shown in Figs. 13 and 14, respectively. These spectra show that the displaced  $\text{H}_2$  gas is readsorbed to form the first and second types of adsorbed hydrogen, which cannot be displaced by nitrogen, and are present in the TPD spectra.

The TPD-adsorption spectra on various catalysts and under different adsorption conditions and the effects of  $\text{N}_2$  coadsorption on the TPD spectra of hydrogen are listed in Table 1.

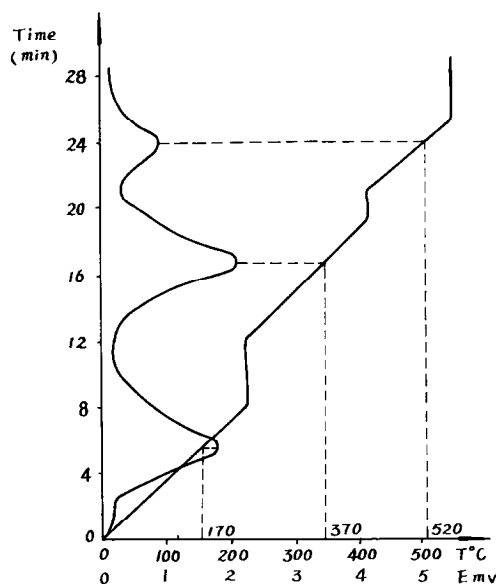


FIG. 10. TPD spectra on catalyst II ( $\text{CaO}-\text{Al}_2\text{O}_3-\text{Fe}$ ) after coadsorption of  $\text{H}_2$  and  $\text{N}_2$  at  $\sim 20^\circ\text{C}$ .

## DISCUSSION

### 1. The Net Charge and Nature of the Three Species of Hydrogen $\text{H}_2^{\delta+}$ , $\text{H}^{\delta+}$ , and $\text{H}^{\delta-}$

As shown by experimental data, adsorbed nitrogen is negatively charged since

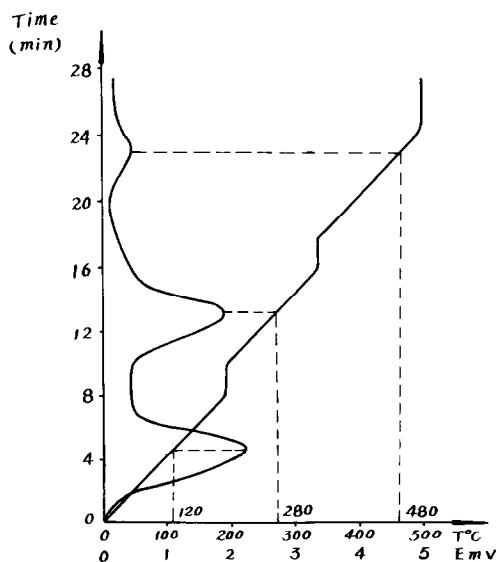


FIG. 11. TPD spectra on catalyst III ( $\text{Al}_2\text{O}_3-\text{Fe}$ ) after coadsorption of  $\text{H}_2$  and  $\text{N}_2$  at  $\sim 20^\circ\text{C}$ .

TABLE I  
TPD Spectra of Adsorbed Hydrogen on Various Catalysts

Adsorption conditions		Catalyst I (K <sub>2</sub> O–CaO–Al <sub>2</sub> O <sub>3</sub> –Fe)	Catalyst II (CaO–Al <sub>2</sub> O <sub>3</sub> –Fe)	Catalyst III (Al <sub>2</sub> O <sub>3</sub> –Fe)
H <sub>2</sub> adsorbed during cooling from 400 to ~20°C	Peak temp.	120, 340, 520°C	120, 285, 520°C	120, 285, 480°C
	Peak area <sup>a</sup>	A <sub>1</sub> > A <sub>2</sub> ≅ A <sub>3</sub>	A <sub>1</sub> ≅ A <sub>3</sub> > A <sub>2</sub>	A <sub>1</sub> ≅ A <sub>2</sub> ≅ A <sub>3</sub>
H <sub>2</sub> adsorption at ~20°C	Peak temp.	300°C	280°C	200, 380°C
	Peak area	A <sub>2</sub>	A <sub>2</sub>	A <sub>2</sub> ≅ A <sub>3</sub>
Coadsorption of H <sub>2</sub> and N <sub>2</sub> at ~20°C	Peak temp.	150, 380, 540°C	170, 370, 520°C	120, 280, 480°C
	Peak area	A <sub>2</sub> > A <sub>1</sub> > A <sub>3</sub>	A <sub>2</sub> ≅ A <sub>1</sub> > A <sub>3</sub>	A <sub>1</sub> ≅ A <sub>2</sub> ≅ A <sub>3</sub>
Adsorbed hydrogen species of high desorption temperature (>540°C) displaced by N <sub>2</sub>	Peak temp.	220, 370°C	130, 300°C	125, 290°C
	Peak area	A <sub>2</sub> > A <sub>1</sub>	A <sub>1</sub> ≅ A <sub>2</sub>	A <sub>1</sub> ≅ A <sub>2</sub>

<sup>a</sup> A<sub>1</sub> = H<sub>2</sub><sup>δ+</sup>, A<sub>2</sub> = H<sup>δ+</sup>, A<sub>3</sub> = H<sup>δ-</sup>.

adsorption of nitrogen causes the work function of iron increase (9) and the resistivity of iron film also increased (3). It is easy to understand that with the great difference in electronegativity between N and Fe, the electron of iron moves to the nitrogen during nitrogen adsorption. That form of adsorbed hydrogen which desorbs at high temperature can be displaced by nitrogen (Fig. 12). The desorption temperature of this form of adsorbed hydrogen is very high (520°C), and its formation is likely to involve a strong covalent bond. The assumption that the hydrogen atom carries a negative charge could explain the displacement of H<sup>δ-</sup> by adsorption of nitrogen. The

desorption peak of H<sup>δ-</sup> form is higher when an N<sub>2</sub> stream is first passed through as shown in Fig. 12. Perhaps this results from a repulsive force between N<sup>δ-</sup> and H<sup>δ-</sup>. There is a large Coulombic repulsion between them if their separation is within the sum of their van der Waals radii, as shown in Fig. 15. Since there is more H<sup>δ-</sup> present when N<sub>2</sub> stream is first passed through, the chance of the repulsion between the two adsorbed species is greater. The repulsion may also be caused by the greater nitrogen adsorption in the early stage of N<sub>2</sub> flushing, at which time more electrons are drawn from H<sup>δ-</sup> promoting H<sup>δ-</sup> desorption. Since the electronegativity of N is greater than

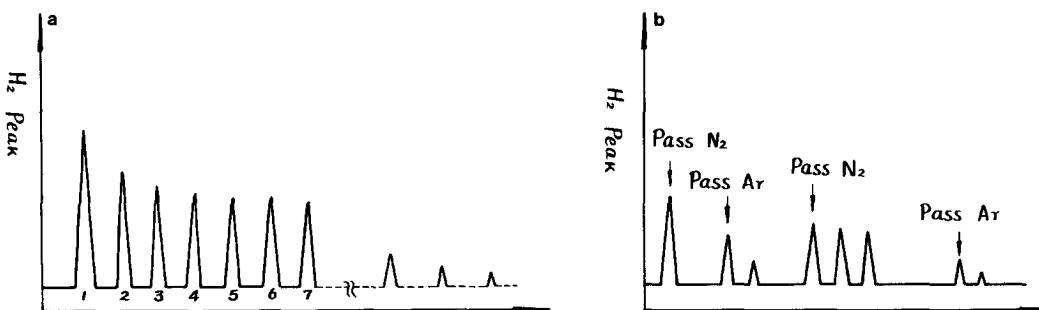


FIG. 12. Displacement of H<sub>2</sub> of high desorption temperature ( $T > 540^{\circ}\text{C}$ ) by N<sub>2</sub> at 410°C. (a) Schematic diagram of change in hydrogen concentration in exit gas with N<sub>2</sub> flushing. (b) Schematic diagram of change in hydrogen concentration in exit gas with alternate passage of N<sub>2</sub> and Ar.

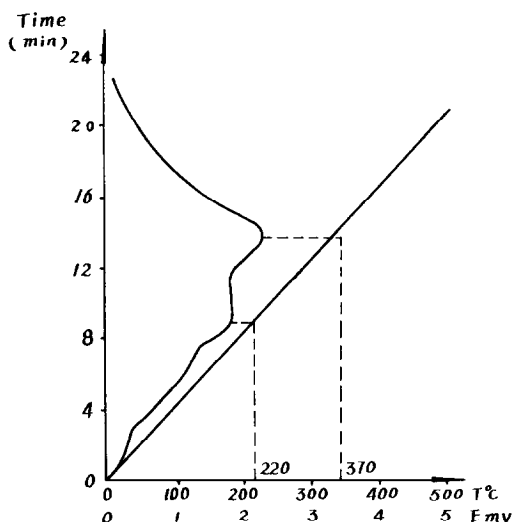


FIG. 13. Adsorbed hydrogen species of high desorption temperature ( $>540^{\circ}\text{C}$ ) replaced by  $\text{N}_2$  at room temperature and TPD of the resulting material. Catalyst I ( $\text{K}_2\text{O}-\text{CaO}-\text{Al}_2\text{O}_3-\text{Fe}$ ).

that of H, N would be the winner in the competition to accept the electron. Thus, negative charge would be transferred from the H atom in  $\text{Fe}-\text{H}^{\delta-}$  to N with the result that the bond in  $\text{Fe}-\text{H}^{\delta-}$  would be weakened and more easily broken. No matter what may be the cause, it appears that the adsorbed hydrogen which desorbed at high temperature is negatively charged.

The weakly adsorbed species of hydrogen which desorb during the first and second peaks in TPD spectra cannot be displaced by nitrogen (see Figs. 13 and 14). The amount of adsorption in these forms is increased when nitrogen is simultaneously adsorbed (compare Figs. 9, 10, and 11 with Figs. 6, 7, and 8, respectively). We assume that the hydrogen adsorbate which desorbed in both of these peaks carried a positive charge. As shown in Fig. 15, there is large Coulombic attraction between the negative  $\text{N}^{\delta-}$  atom and the positive  $\text{H}^{\delta+}$  atom when the distance between them is within the sum of their van der Waals radii. The temperature of the first desorption peak is  $120-170^{\circ}\text{C}$ , whereas that of the second is  $280-380^{\circ}\text{C}$ . The large difference in

temperature between these two peaks is likely caused not by heterogeneous surface sites but rather by the nature of different chemical species, for example,  $\text{H}_2^{\delta+}$  and  $\text{H}^{\delta+}$ . The adsorption bond strength of  $\text{H}_2^{\delta+}$  is weaker than that of  $\text{H}^{\delta+}$ , and the desorption temperature of  $\text{H}_2^{\delta+}$  ( $120^{\circ}\text{C}$ ) is not much more than the boiling point of water.

Is it possible that charge transfer occurs directly from  $\text{H}^{\delta-}$  to form  $\text{H}^{\delta+}$  and  $\text{N}^{\delta-}$ ? In Fig. 13 the peak area of  $\text{H}_2^{\delta+}$  is large, even if we assume  $\text{H}^{\delta-} \rightarrow \text{H}^{\delta+}$ , but at room temperature  $\text{H}^{\delta+}$  is not desorbed and cannot change into  $\text{H}_2^{\delta+}$  (see Fig. 6). How can we explain that the stronger type  $\text{H}^{\delta+}$  can change into the weaker type  $\text{H}_2^{\delta+}$  at a temperature which is below that of desorption of  $\text{H}^{\delta+}$ ? To change  $\text{H}^{\delta-}$  (desorption temperature peak  $520^{\circ}\text{C}$ ) to  $\text{H}^{\delta+}$  (desorption temperature peak  $280$  to  $380^{\circ}\text{C}$ ) by electron transfer requires a large amount of energy (reflected by the large difference between the temperatures of the peaks). The electron accepted by nitrogen comes almost totally from iron while only a small part comes from  $\text{H}^{\delta-}$  through iron. It might be impossible to form  $\text{H}^{\delta+}$  from  $\text{H}^{\delta-}$  by transfer of charge between  $\text{H}^{\delta-}$  and N. There-

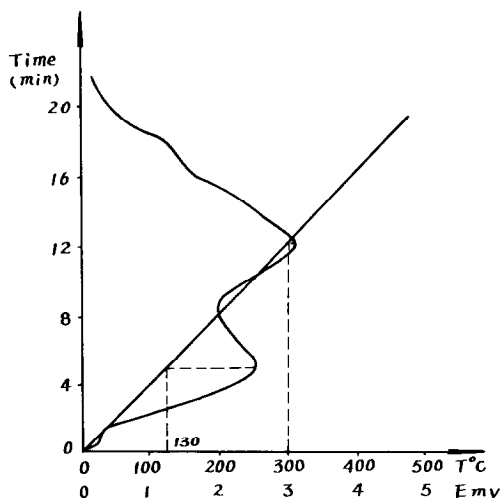


FIG. 14. Adsorbed hydrogen species of high desorption temperature ( $>540^{\circ}\text{C}$ ) replaced by  $\text{N}_2$  at room temperature and TPD of the resulting material. Catalyst II ( $\text{CaO}-\text{Al}_2\text{O}_3-\text{Fe}$ ).



fore, in the case of Fig. 13, it is more likely that the strong adsorption bond of  $\text{Fe}-\text{H}^{\delta-}$  is weakened with resulting desorption as  $\text{H}_2$  (gas) when the nitrogen is passed through the catalyst bed and that the gaseous hydrogen is then readsorbed onto the surface to form  $\text{H}^{\delta+}$  and  $\text{H}_2^{\delta+}$  on iron sites neighboring the promoter.

## 2. The Effect of Promoters

From the TPD spectra on the  $\text{Fe}-\text{K}_2\text{O}-\text{CaO}-\text{Al}_2\text{O}_3$  catalyst (I) and  $\text{K}_2\text{O}$ -free catalysts (II and III), we observed that the temperature for the desorption peak of  $\text{H}^{\delta+}$  increases from 285 to 340°C (see Figs. 3, 4, and 5). The peak area of  $A_{\text{H}^{\delta+}}/A_{\text{H}_2^{\delta+}}$  also increases, obviously due to the  $\text{K}_2\text{O}$  component.

The dissociation of  $\text{H}_2$  to form  $\text{H}^{\delta+}$  may occur in two ways, by heterolytic splitting of  $\text{H}_2$  to form  $\text{H}^{\delta+}$  and  $\text{H}^{\delta-}$ , or by homolytic splitting to form  $2\text{H}^{\delta+}$ . The former path seems more probable, although both are promoted by a dipole promoter. Therefore, the increase in the amount of  $\text{H}^{\delta+}$  is more remarkable on  $\text{K}_2\text{O}-\text{CaO}-\text{Al}_2\text{O}_3-\text{Fe}$ .

The depression of the exit work function by adding  $\text{K}_2\text{O}$  may favor formation of  $\text{H}^{\delta-}$  and  $\text{N}_2^{\delta-}$  and  $\text{N}^{\delta-}$ . If we include the hydrogen which desorbs at  $T > 540^\circ\text{C}$  in the total amount of  $\text{H}^{\delta-}$ ,  $\text{H}^{\delta-}$  is the most abundant species. From the preliminary results, the amount of  $\text{H}^{\delta-}$  on the various catalysts is I

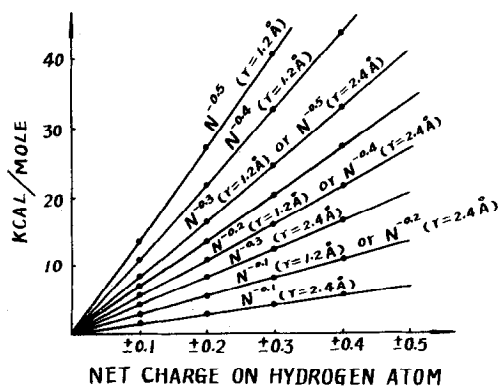


FIG. 15. The Coulombic energy between  $\text{N}^{\delta-}$  and  $\text{H}^{\delta+}$  in relation to atomic net charges (interatomic distance  $\text{N}-\text{H}$  shown in parentheses).

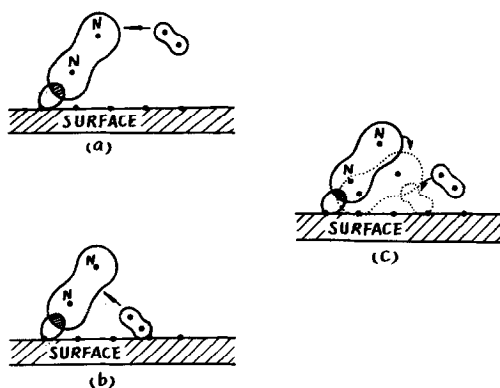


FIG. 16. Schematic representation of mechanisms of surface reaction.

$> \text{II} > \text{III}$ . This clearly shows that the smaller the exit work function of the catalyst, the larger the amount of  $\text{H}^{\delta-}$ .

Since the  $\text{K}_2\text{O}$  promoter has a large dipole, it may also be favorable for forming  $\text{H}^{\delta+}$ . The dipole effect is particularly remarkable in the coadsorption of  $\text{N}_2$  and  $\text{H}_2$  as discussed below.

## 3. The Coadsorption of $\text{N}_2$ and $\text{H}_2$

Comparing Figs. 9, 10, and 11 with Figs. 6, 7, and 8, respectively, we find that there are remarkable differences in the TPD spectra between  $\text{H}_2$  adsorbed alone and  $\text{H}_2$  adsorbed in conjunction with  $\text{N}_2$  on the same catalyst, at room temperature, and with the same pretreatment conditions. First, the amount of adsorbed  $\text{H}_2^{\delta+}$  and  $\text{H}^{\delta+}$  increase greatly with nitrogen adsorption. Second, the temperature of the desorption peak of  $\text{H}^{\delta+}$  increases greatly with nitrogen adsorption. For example, on catalyst I, it increased from 300 to 380°C, on catalyst II from 280 to 370°C, and on catalyst III from 200 to 280°C. Third, the greater the dipole moment of catalyst, the higher the desorption temperature.

The energy of the dipole-dipole reaction can be calculated by

$$E_{\text{dipole-dipole}} = \frac{\mu_a \mu_b}{R^3} (2\cos \theta_a \cos \theta_b + \sin \theta_a \sin \theta_b \cos \phi),$$

where  $\mu_a$  and  $\mu_b$  are the dipole moment of a and b,  $R$  is the distance between two dipole centers;  $\theta_a$  and  $\theta_b$  are the angles between the  $z$  axis and dipoles a and b;  $\varphi$  is the angle between the planes of dipoles a and b. The results are shown in Table 2. The dipole of a promoter such as  $K^+ AlO_2^-$  or  $K^+ FeO_2^-$  may interact with the dipole  $N^{\delta-} \cdots H^{\delta+}$  to lower the energy of the system. The dipole-dipole interaction energy is not small if the distance between the  $N^{\delta-}$  and  $H^{\delta+}$  is within the sum of their van der Waals radii. Therefore, the desorption temperature of  $H^{\delta+}$  increases greatly.

$H^{\delta-}$  behaves in the reverse manner. The desorption peak of  $H^{\delta-}$  adsorbed alone does not appear in Fig. 6 because it is higher than 550°C. But this does appear in Fig. 9 which is the spectrum of simultaneous adsorption of  $N_2$  with  $H_2$ . As described above, the adsorption of nitrogen is a process by which an electron would be drawn from iron. The  $Fe-H^{\delta-}$  bond will be

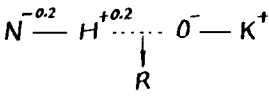
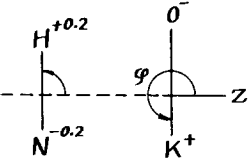
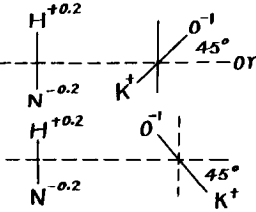
weakened, resulting in a decrease in the desorption temperature.

Comparing Figs. 3, 4, and 5 with Figs. 9, 10, and 11, respectively, we find that if the hydrogen is coadsorbed with nitrogen on the same catalyst at room temperature, the desorption peaks of  $H_2^{\delta+}$ ,  $H^{\delta+}$  increase from 120, 340 to 150, and 380°C on the catalyst I, and from 120, 285 to 170, and 370°C on the catalyst II, respectively. Here the dipole-dipole interaction is important. The larger the dipole moment the greater the increase in the desorption temperature. The dipole moment of  $Fe-Al_2O_3$  catalyst (No. III) is small; so its behavior is quite different.

#### 4. Estimation of Adsorption Heats and Adsorption Equilibrium Constants of $H_2^{\delta+}$ , $H^{\delta+}$ , and $H^{\delta-}$

The statistical entropy of  $H_2$  at 1 atm and  $S_{vib}^\circ$  of adsorption species can be estimated

TABLE 2  
The Energy of Dipole-Dipole Mutual Reaction

Dipoles	$R^a$ (Å)	$\Delta E$ Dipole <sup>b</sup> (Kcal/mol)	Notes	
	2	-60.2	The sum of van der Waal's radii between O and H equals 2.64 Å	
	3	-17.8		
	4	-7.5		
	5	-3.9		
	2	-30.1	$\varphi$	$\Delta E^c$
	3	-8.9	0°	-8.9
	4	-3.8	45°	-6.3
	5	-1.9	90°	0
			135°	+6.3
			180°	+8.3
	2	-2.3	0°	-6.3
	3	-6.3	45°	-4.9
	4	-2.7	90°	0
	5	-1.4	135°	+4.9
			180°	+6.3

<sup>a</sup> Distance between two dipole centers and assuming the distance between  $N^{\delta-}$  and  $H^{\delta+}$  is 1.05 Å.

<sup>b</sup> For  $\varphi = 0$ .

<sup>c</sup> For  $R = 3.0$  Å,  $\varphi$  at various values.

according to the formulas

$$S_{\text{tran}}^{\circ} = 4.9680 + 6.8635 \log M \\ + 11.4392 \log T - 7.2820,$$

$$S_{\text{rot}}^{\circ} = 1.9872 + 4.5757 \log (I \\ \times 10^{39}) + 4.5757 \log T \\ - 4.5757 \log \sigma + 2.7676,$$

$$S_{\text{vib}}^{\circ} = 1.9872 \sum_i x_i / (e^{x_i} - 1) \\ - 1.9872 \sum_i \ln(1 - e^{x_i}),$$

where  $x_i = \nu_i hc/kT$ , and  $\nu_i$  is the fundamental frequency ( $\text{cm}^{-1}$ ). Assume that

$$\nu_{\text{H-H}} = 4405 \text{ cm}^{-1}, \nu_{\text{Fe-H}_2^{\delta+}} = 500 \text{ cm}^{-1}, \\ \nu_{\text{Fe-H}^{\delta+}} = 1200 \text{ cm}^{-1},$$

$$\nu_{\text{Fe-H}^{\delta-}} = 1700 \text{ cm}^{-1}.$$

Because the value of  $S_{\text{vib}}^{\circ}$  is usually 0.1–2% of  $(S_{\text{tran}}^{\circ} + S_{\text{rot}}^{\circ})$  of gas, the error of the estimation of vibration frequency has little on the total entropy change of adsorption. From

$$S^{\circ} = S_{\text{tran}}^{\circ} + S_{\text{rot}}^{\circ} + S_{\text{vib}}^{\circ},$$

$$(\Delta S^{\circ})_{\text{ads}} = (S^{\circ})_{\text{ads}} - (S^{\circ})_{\text{gas}},$$

$$\Delta Z^{\circ} = \Delta H^{\circ} - T \Delta S^{\circ} = -RT \ln K_p,$$

we can calculate  $K_p$  if certain  $\Delta H^{\circ}$  values and adsorption models are assumed. The results are shown in Tables 3A and B. The immobile adsorption is assumed and, thus,  $S_{\text{tran}}^{\circ}$  and  $S_{\text{rot}}^{\circ}$  of adsorption are equal to zero, and in mobile adsorption it is assumed that  $S_{\text{tran}}^{\circ}$  and  $S_{\text{rot}}^{\circ}$  are equal to one-third of  $S_{\text{tran}}^{\circ}$  and  $S_{\text{rot}}^{\circ}$  of the gas. The actual adsorption states may be intermediate between these two extremes.

From Tables 3A and B and the temperatures of the desorption peaks (120, 340, 520°C) corresponding to  $\text{H}_2^{\delta+}$ ,  $\text{H}^{\delta+}$ ,  $\text{H}^{\delta-}$ , respectively, we can estimate the values of the heats of adsorption of  $\text{H}_2^{\delta+}$ ,  $\text{H}^{\delta+}$ ,  $\text{H}^{\delta-}$  to be 5–10, 10–15, and larger than 15 Kcal/mol, respectively.

The heat of adsorption of  $\text{H}_2$  at high temperature on a doubly promoted catalyst obtained by Kwan (10) (5–10 Kcal/mol) agrees with our results.

TABLE 3A  
The Adsorption Equilibrium Constant of Hydrogen Adsorbed in an Immobile Form

Adsorption heat, $Q_p$ (kcal/mol)	120°C			340°C			520°C		
	$\text{H}_2^{\delta+}$	$\text{H}^{\delta+}$	$\text{H}^{\delta-}$	$\text{H}_2^{\delta+}$	$\text{H}^{\delta+}$	$\text{H}^{\delta-}$	$\text{H}_2^{\delta+}$	$\text{H}^{\delta+}$	$\text{H}^{\delta-}$
5.0	$3.91 \times 10^{-6}$			$8.49 \times 10^{-8}$			$1.38 \times 10^{-8}$		
10.0	$2.27 \times 10^{-3}$	$1.54 \times 10^{-3}$		$5.02 \times 10^{-6}$	$4.82 \times 10^{-6}$		$3.00 \times 10^{-7}$	$4.26 \times 10^{-7}$	
15.0		$8.96 \times 10^{-1}$			$2.85 \times 10^{-4}$			$8.99 \times 10^{-6}$	
20.0			$4.68 \times 10^2$			$1.26 \times 10^{-2}$			$1.56 \times 10^{-4}$
25.0			$2.72 \times 10^5$			$7.46 \times 10^{-1}$			$3.66 \times 10^{-3}$
30.0			$1.58 \times 10^8$			$4.42 \times 10^1$			$6.66 \times 10^{-1}$
35.0			$9.17 \times 10^{10}$			$2.62 \times 10^3$			$2.01 \times 10^0$

TABLE 3B  
The Adsorption Equilibrium Constant of Hydrogen Adsorbed in a Mobile Form

Adsorption heat, $Q_p$ (kcal/mol)	120°C			340°C			520°C		
	$H_2^{\delta+}$	$H^{\delta+}$	$H^{\delta-}$	$H_2^{\delta+}$	$H^{\delta+}$	$H^{\delta-}$	$H_2^{\delta+}$	$H^{\delta+}$	$H^{\delta-}$
5.0	$2.46 \times 10^{-3}$	$1.67 \times 10^{-3}$		$8.95 \times 10^{-5}$	$8.59 \times 10^{-5}$		$1.95 \times 10^{-5}$	$2.57 \times 10^{-5}$	
10.0	$1.43 \times 10^0$	$9.72 \times 10^{-1}$		$5.30 \times 10^{-3}$	$5.08 \times 10^{-3}$		$4.60 \times 10^{-4}$	$6.04 \times 10^{-4}$	
15.0			$5.07 \times 10^2$			$2.23 \times 10^{-1}$			$9.44 \times 10^{-3}$
20.0			$2.95 \times 10^5$			$1.33 \times 10^1$			$2.22 \times 10^{-1}$
25.0			$1.71 \times 10^8$			$7.87 \times 10^2$			$5.19 \times 10^0$
30.0			$9.95 \times 10^{10}$			$4.66 \times 10^4$			$1.22 \times 10^3$
35.0			$5.78 \times 10^{13}$			$2.76 \times 10^6$			$2.85 \times 10^3$

From the  $\Delta H$  of  $H_2^{\delta+}$ ,  $H^{\delta+}$ , we can calculate  $K_p$  at various temperature. At the reaction temperature of ammonia synthesis,  $(K_p)_{H_2^{\delta+}}$  and  $(K_p)_{H^{\delta+}}$  are much less than  $10^{-3}$ . It is obvious that  $(K_{H_2P_{H_2}})_{H_2^{\delta+}}$  and  $(K_{H_2P_{H_2}})_{H^{\delta+}}$  are much less than unity, which is an important assumption in our derived equation (1b).

### 5. The Nature of the Adsorbed Species and the Mechanism of Ammonia Synthesis

In spite of many efforts to determine the relationship between the nature of the adsorption of hydrogen on a catalyst and its activity for ammonia synthesis, the problem is still unresolved.

In order to elucidate the mechanism of a heterogeneous reaction, one of the most important things is, as Tamaru said: "The amount of adsorption and the nature and structure of each of the surface species under the reaction conditions should be examined and the rate of the reaction of each should be compared to the rate of the overall reaction."

If the amount of hydrogen adsorption would include all species desorbing at high temperature, the most abundant adsorbed species would be inactive  $H^{\delta-}$ . Therefore, we cannot determine the relationship between activity and the total amount of adsorption, as found by Tamaru (7) and Topsøe *et al.* (8).

The TPD spectra of coadsorbed  $N_2$  and  $H_2$  shows that catalyst I exhibits the largest desorption peak area for  $H^{\delta+}$  (Figs. 9–11). Catalyst I is also the most active one. Therefore, there may be a rate-controlling step in the reaction path, similar to that of nitrogen adsorption promoted by  $H^{\delta+}$ . This controlling step may also proceed by a promoter dipole.

Many experimental facts show that the concentration of adsorbed  $N_2$  is very small at reaction temperature. This is confirmed by TPD of adsorbed  $N_2$  (see Part II). However, Ertl (11) observed that the rate of dis-

sociation of adsorbed  $N_2$  is much lower than that of the molecular adsorption of  $N_2$ . The dissociation of adsorbed  $N_2^{\delta-}$  is thus possibly a rate-controlling step. We have proposed a structure model for the dissociation of adsorbed  $N_2$  with the help of the coadsorbed  $H^{\delta+}$  onto the  $\alpha$ -Fe(111) plane which has been checked by the EHMO method (1, 12).

It is necessary to point out that (a) hydrogen adsorption on iron atoms can be induced by a negatively charged atom or dipole in the vicinity of the adsorbed hydrogen to form  $H_2^{\delta+}$  and  $H^{\delta+}$ ; (b) the adsorbed  $N^{\delta-}$  has the ability to induce hydrogen to form  $H^{\delta+}$  or  $H_2^{\delta+}$ , if hydrogen is adsorbed in the vicinity of  $N^{\delta-}$ ; (c)  $H_2^{\delta+}$  and  $H^{\delta+}$  are weakly chemisorbed species of a small heat of adsorption; (d) no matter how  $H^{\delta+}$  is formed, the  $(K_{H_2}P_{H_2})_{H^{\delta+}}$  and  $(K_{H_2}P_{H_2})_{H_2^{\delta+}}$  are much less than unity.

A kinetic equation based on the formation of  $N_2^{\delta-}$  and the hydrogenation of  $N_2^{\delta-}$  to form  $NH_x$  ( $x = 0, 1, 2$ ), and the assumption of  $(K_{H_2}P_{H_2})_{H^{\delta+}} \ll 1$  has been derived and proven (1b, 14).

We assume there are two possible adsorbed states of dinitrogen, as shown in Fig. 16c. The inclined angle of the dinitrogen molecule of the first adsorbed state onto the  $\alpha$ -Fe(111) plane is larger than that of the second adsorbed state. The first adsorbed state reaches equilibrium at a very fast rate, but its coverage is very low. The dissociation of the dinitrogen molecule requires that the first state be transferred to the second state, so that the triple bond of dinitrogen can be weakened by side-on coordination of iron cluster and the  $exo-N^{\delta-}$  of dinitrogen can be reacted with two  $H^{\delta+}$  which are adsorbed on both sides of dinitrogen (dipole reaction). This process is a rate-controlling step. Because the adsorption equilibrium constant of the first adsorbed state is very small at reaction temperature, the formal kinetic expression of the elementary step which results in the transformation of the first adsorbed state to the second adsorbed state is the same as that of the

elementary step which leads from  $N_2$  gas directly to the second adsorbed state.

If helium gas is used instead of argon, the desorption peaks of  $N_2^{\delta-}$  and  $N^{\delta-}$  are observed in the TPD spectra. The peak of  $N^{\delta-}$  occurs above  $550^\circ\text{C}$ , and that of  $N_2^{\delta-}$  below  $-120^\circ\text{C}$ . The peak area of  $N_2^{\delta-}$  is larger when  $N_2$  and  $H_2$  are coadsorbed as compared with the case of adsorption of  $N_2$  alone. The details of this will be discussed in Part II. The dynamically induced mode of  $N_2^{\delta-} \cdots 2H^{\delta+}$  at high temperature may be a transition state, at the top of the potential energy curve, or a highly unstable adsorbed state. It cannot be detected directly by this method, but it can be recognized from the behavior of hydrogen adsorption, the  $N_2^{\delta-} \cdots H^{\delta+}$  coadsorption at low temperature, and the dynamic behavior of  $N_2^{\delta-}$ . The mechanism of  $N_2^{\delta-}$  hydrogenation, as shown in Fig. 16c is different from the mechanism shown in Fig. 16a, because hydrogen gas does not react directly with adsorbed  $N_2^{\delta-}$  but reacts with  $N_2^{\delta-}$  through a transient state on a vacant iron site, or nitrogen gas reacts with adsorbed  $H^{\delta+}$  through a transient state on another vacant iron site, or both  $N_2$  and  $H_2$  simultaneously pass through their transient states and react with each other. Thus, it also does not follow the mechanism shown in Fig. 16b, where the first adsorbed  $N_2^{\delta-}$  state must change to the second adsorbed state before reacting with adsorbed  $H^{\delta+}$ .

#### ACKNOWLEDGMENTS

The authors thank Mr. Wei Ke Mei (Fuchow University) for the preparation of catalyst, Mr. Wu Wei Heng (Xiamen University, Foreign Languages Department) for his help with the manuscript, and valuable discussions with Professor K. R. Tsai (Xiamen University).

#### REFERENCES

1. Huang, K. H., (a) "Proceedings, 7th International Congress on Catalysis," p. 554, 1981; (b) *Sci. Sin.* **24**, No. 6, 800 (1981); (c) *Universitatis Amoiensis (Acta Sci. Natur.)* **3**, 112, 130 (1978); (d) Li, J. T. *et al.*, to be published.
2. (a) Bond, G. C., "Catalysis by Metals," p. 97 (1962); (b) Harkness, R. W., and Emmett, P. H.,

- J. Amer. Chem. Soc.* **56**, 490 (1931); (c) Emmett, P. H., and Harkness, R. W., *J. Amer. Chem. Soc.* **57**, 1631 (1935); (d) Kummer, J. T., and Emmett, P. H., *J. Phys. Chem.* **56**, 258 (1952).
3. Wedler, G., and Borgmann, D., (a) *J. Catal.* **44**, 139 (1976); (b) *Surf. Sci.* **100**, 507 (1980).
4. Amenomiya, Y., and Pleizier, G., *J. Catal.* **28**, 442 (1973).
5. (a) Brunauer, S., and Emmett, P. H., *J. Amer. Chem. Soc.* **62**, 1732 (1940); (b) Podgurski, H. H., and Emmett, P. H., *J. Phys. Chem.* **57**, 159 (1953).
6. Bokhoven, C., Zwitering, P., *et al.*, in "Advances in Catalysis," Vol. III, pp. 313, 316, 317. Academic Press, New York, 1955.
7. Tamaru, K. *et al.* (a) *Bull. Chem. Soc. Japan* **31**, 666 (1958); (b) "Proceedings, 3th International Congress on Catalysis," p. 664 (1964).
8. Topsøe, H., Topsøe, N., Bohlbro, H., and Dumesic, J. A., "Proceedings, 7th International Congress on Catalysis," p. 247, 1981.
9. Brill, R., *et al.*, (a) *Angew. Chem. (Int. Ed.)* **6**, 882 (1967); (b) *Z. Phys. Chem.* **64**, 215 (1969); (c) *J. Catal.* **16**, 16 (1970).
10. Kwan, T., *J. Res. Inst. Catal. Hokkaido Univ.* **1**, 100 (1949).
11. Ertl, G., (a) Proceedings, 7th International Congress on Catalysis," p. 21, 1981; (b) *Catal. Rev.-Sci. Eng.* **21** (2), 201 (1980).
12. Huang, K. H., Zeng, X. M., Lai, W. J., and Li, J. T., "Parameter Selection of EHMO Calculation to Qualitatively Discriminate Adsorption Models of Transition Metal Clusters," presented at 182nd ACS National Meeting, New York, Aug. 27, 1981.
13. Temkin, M. E., *et al.*, *Kinet. Catal. USSR* **4**, 260, 563 (1963).
14. Liu, D. M., Zhao, Z. L., Huang, Z. X., and Wu, X. J., *J. Chem. Eng. China* **2**, 133 (1979).